UCRL-53597

Petite Sismique Measurements at the Spent Fuel Test—Climax

J. J. Zucca

September 1984

Lawrence Livermore National Laboratory

Work performed under the auspices of the U.S. Department of Energy by Lawrence Livermore National Laboratory under Contract W-7405-Eng-48.

UCRL-53597
Distribution Category UC-70

Petite Sismique Measurements at the Spent Fuel Test—Climax

J. J. Zucca

Manuscript date: September 1984

LAWRENCE LIVERMORE NATIONAL LABORATORY
University of California • Livermore, California • 94550

Available from: National Technical Information Service • U.S. Department of Commerce
5285 Port Royal Road • Springfield, VA 22161 • $8.50 per copy • (Microfiche $4.50)

Contents

Petite Sismique Measurements at the Spent Fuel Test—Climax

Abstract

In May 1984, a "petite sismique" estimate of the deformation modulus (E) was carried out at the Spent Fuel Test—Climax (SFT—C) at the Nevada Test Site. The first part of the experiment was to repeat an earlier suite of measurements that were taken before the spent fuel was emplaced to see if any changes had resulted from heating the rock mass. The results of this measurement indicate a decrease in the modulus. However, these results are suspect in view of the findings in the second part of the experiment, which was designed to minimize the effects due to spurious resonances in the source and geophone locations. These effects were thought to bias the earlier measurements. The measurements indicate that the rock acts as a low-pass filter to the propagating wavefield. Furthermore, it is noted that the blow from a hammer is not a purely impulsive source. Therefore, depending on the type of source used and the distance away from the source, a different peak frequency and, hence, E could be measured for the same rock mass. Unless these effects are somehow factored out of a petite sismique survey, the value of E obtained could be severely biased.

Introduction

The petite sismique method was originally proposed by Schneider (1967) as a means of rapidly determining the *in-situ*, static, field deformation modulus (E) of a rock mass. Since the original study, Bieniawski (1978) has reported additional results. The petite sismique technique involves striking the rock mass in some way to create a shear wave and then recording the signal at some location up to tens of meters away. The dominant frequency of the recorded S-wave is measured and the result used to find the modulus through the use of an empirical relationship shown in Fig. 1. The combined data of Schneider (1967) and Bieniawski (1978) as compiled by Heuze et al. (1981) are represented in the figure. These data were produced by first taking a petite sismique measurement and then measuring the field modulus in some other fashion, such as with a flat jack, to provide the empirical relationship between E and the peak frequency.

The petite sismique technique is interesting because it is relatively inexpensive and easy to perform compared with the flat-jack and plate tests. The technique was originally used at the SFT—C as part of an effort to measure E by many different methods (Heuze et al., 1981). In this study, the average dominant frequency of the S-waves recorded was 1100 Hz, which yielded a modulus of 50 GPa.

Since the time of this original study, several questions have arisen concerning the validity of these results. Shake-table tests demonstrated that the geophones used had large peaks in the high end of their response curves that were near the observed peak frequencies. This raised the possibility that the observed peak frequencies were biased by the instrument response. Another problem was with the shear-wave sources used. Although several sources were investigated, most records resulted from a sideways blow with a 4-lb hammer against a stack of steel plates secured to the rock surface with a bolt. It is possible that the 1.8- to 2.4-m-long bolts could have resonated, which would have also tended to bias the peak frequency measured at the geophone.

The original petite sismique measurements were made before the spent nuclear fuel assemblies were emplaced and stored. The spent fuel assemblies and electrical heaters raised the rock mass temperature from the ambient 23°–30°C to

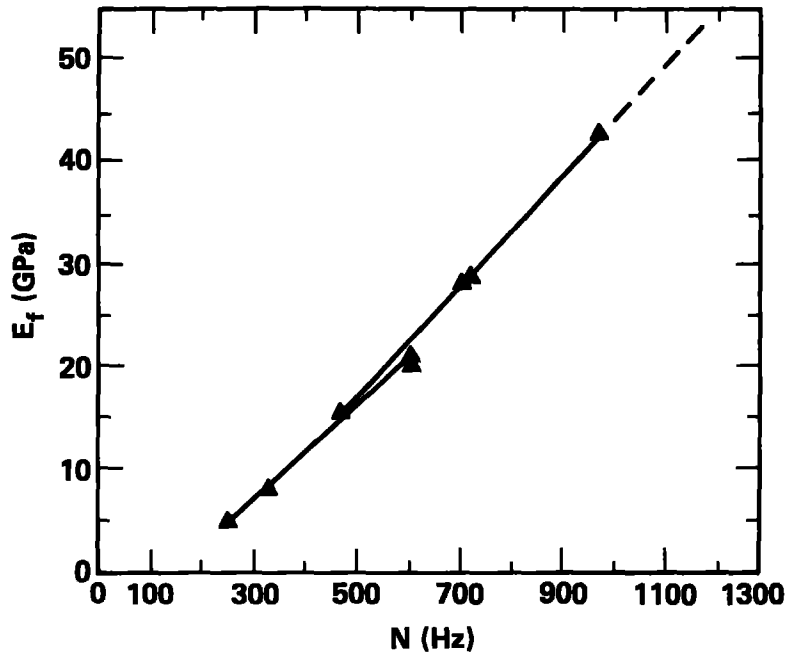

Figure 1. Empirical relationship between the peak frequency of the S-wave and the static *in-situ* modulus of igneous rock masses. (after: Hueze et al., 1981).

85°C at locations throughout the test array (Patrick et al., 1982). After the fuel was removed and the rock mass cooled, the question naturally arose as to whether the rock modulus had changed as a result of the elevated temperature. It was decided to return to the mine to repeat the petite sismique survey to see if any change had occurred and to try to address the problems of the original survey.

Experimental Procedure

The layout of the Climax mine and the source and receiver points for the first part of the experiment are shown in Fig. 2a. The same source and receiver points were occupied as reported in Heuze et al. (1981). However, it is uncertain whether the geophones used had the same response characteristics as in the previous study. In that study, three model GH-3-14 geophones were leased from EG&G and are no longer available commercially. According to information obtained from EG&G, the GH-3-14 geophone was manufactured by several companies for EG&G Geometrics. For the current study, a Geosource model SM-7 geophone was used, which, according to EG&G, has approximately the same frequency response as the GH-3-14 geophone. This uncertainty is especially critical in light of the problem, discussed more fully below, of geophone response to frequencies much greater than the natural frequency.

To record the data throughout the experiment, an EG&G Geometrics ES1210F, 12-channel, signal-enhancing seismograph with a polarity-reversing switch on the geophone input was used. The seismograph triggers on the hammer blow, digitizes the incoming signal, and displays it on a screen in the field. The signal-enhancing feature allows repeated strikes of the hammer to be stacked at the same source to suppress noise. A polarity-reversing switch is also used to suppress the P-wave contribution to the signal. The data are then transmitted to cassette tape on a separate box in the field and the seismograph is ready to record the next source. The cassette tapes are played back into the main computer in the office for processing.

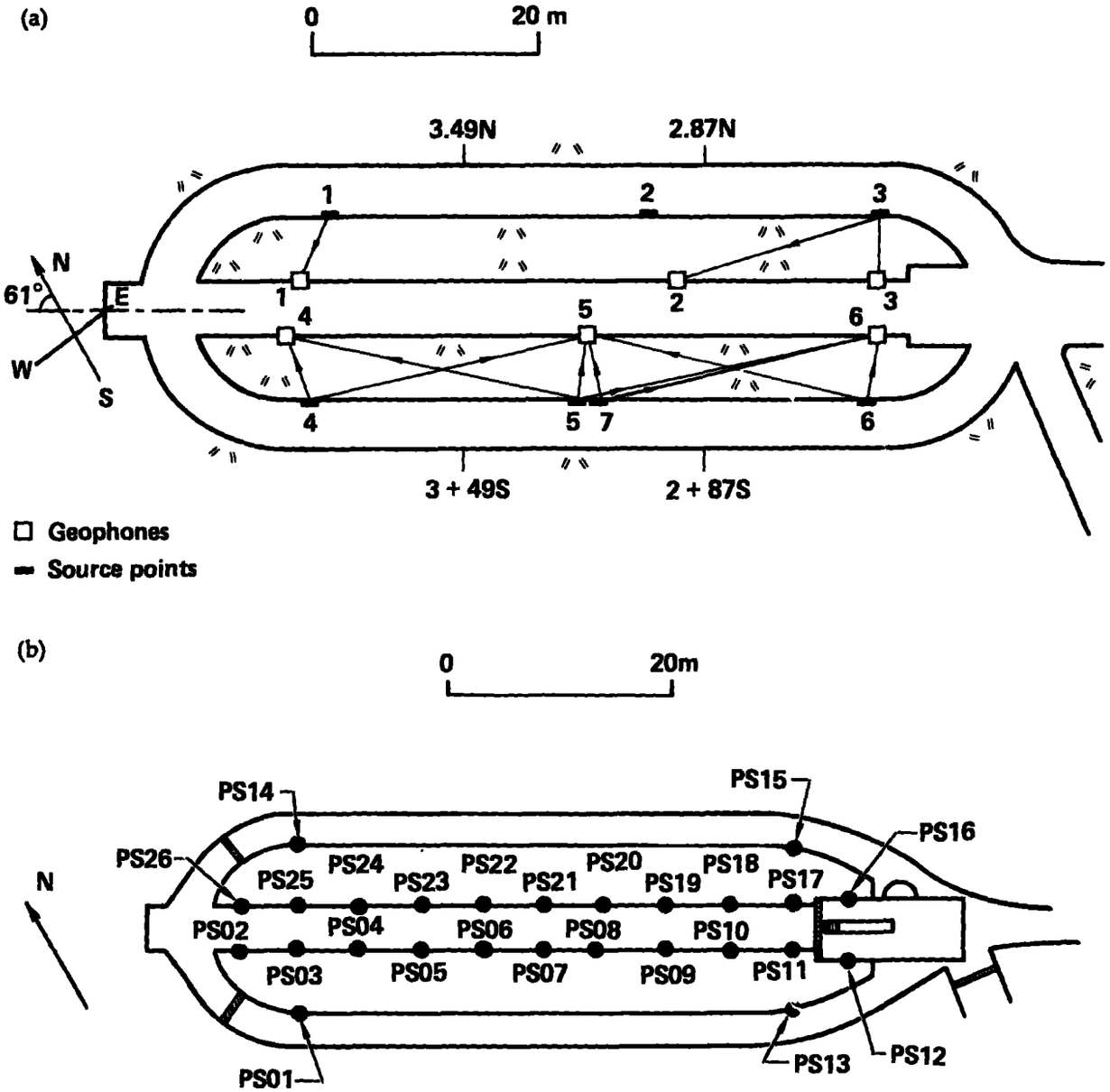

Figure 2. Map-view of the Spent Fuel Test—Climax. (a) Source and receiver locations for the first part of the experiment; (b) receiver locations for the second part of the experiment. The sources were located in the outside drifts at receiver locations PS01, PS13, PS14, and PS15.

For the first part of the experiment, the Geosource model SM-7 geophone was mounted on stainless steel rods that were glued into 0.95-cm-diameter holes drilled into the pillars of the mine. The geophone recorded the horizontal component of motion parallel to the rock face of the pillar. Only one geophone was used for this part of the experiment.

For the second part of the experiment, a more elaborate field setup was used (Fig. 2b). The goal was to minimize the resonance effects of the source and receiver points. AMF-Geospace model GS-11D geophones were used throughout, and 12 channels of data were recorded at once. Figure 3 illustrates the mounting procedure of the geophones. A block of aluminum 6.4 cm on a side

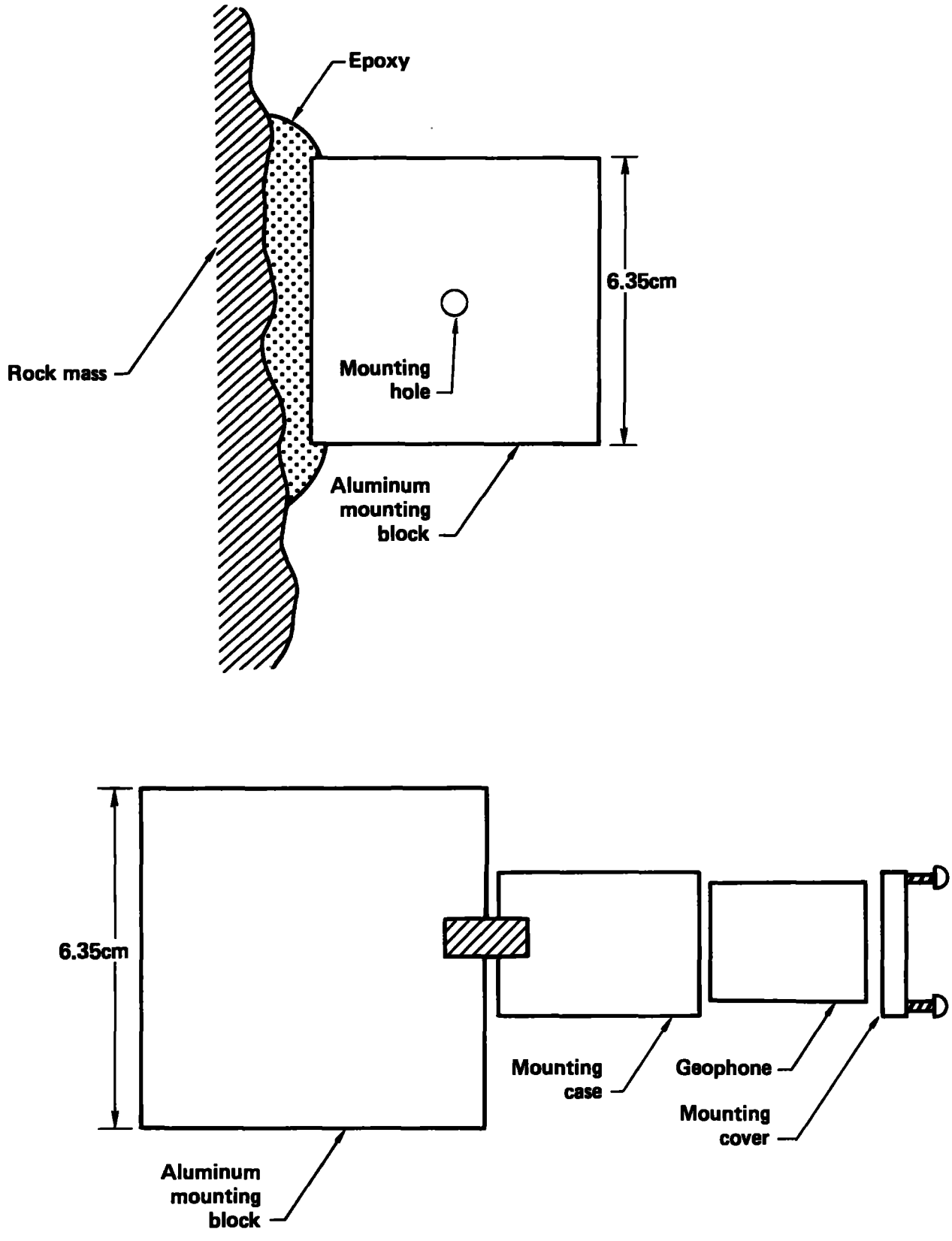

Figure 3. Schematic diagram showing the method of geophone mounting to the rock wall.

was glued to the wall with epoxy and held level while the glue set. The surface of the block facing the wall was roughened and treated with a special coating to better enhance adhesion. The geophone was then set in an aluminum holder that was fastened to the block by means of a set screw. The idea of the mount was to minimize spurious resonances that could be caused by having the geophone suspended away from the rock on a steel rod.

Two different types of sources were used, again with the emphasis on minimizing spurious resonances. The "wood/jack" turned out to provide the best data. It consisted of two blocks of wood approximately 30 cm on a side that were jacked between the two walls of the drift (Fig. 4). The side of the wood was struck with a 1.8-kg hammer to produce S-waves. The other source was an aluminum block (referred to as al-block) approximately 6.4 x 6.4 x 25.0 cm. The block was glued to the wall with the same epoxy that was used for the geophone mounting blocks and was rapped along the long axis with a small lead hammer to produce shear waves. Figure 5 shows recordings and spectra from the wood/jack and al-block sources on model GS-11D geophones. Note that the dominant frequency produced by the wood/jack (~350 Hz) is significantly lower than the dominant frequency produced by the al-block (~4400 Hz). Note also that the al-block resonates much more than the wood/jack. The al-block signal has at least 22 peaks before the signal falls off into the noise. The wood/jack has only seven peaks before its signal enters the noise. The fact that the wood/jack source did not resonate so much and that it could be hit very hard to impart a large signal to the rock made it superior to the al-block.

Geophone Response

As mentioned above, an important consideration is the response of the geophone to high frequencies. Most geophones have large peaks in their response spectra that could lead to biased results. In the first part of the experiment, a Geosource SM-7 geophone was used. The frequency response of this geophone to constant velocity with critical damping is shown in Fig. 6. The response is flat above the natural frequency of 14 Hz to about 1 kHz, where it begins to peak. A strong peak occurs in the response curve at 1.6 kHz. Unfortunately, it is not clear if this curve

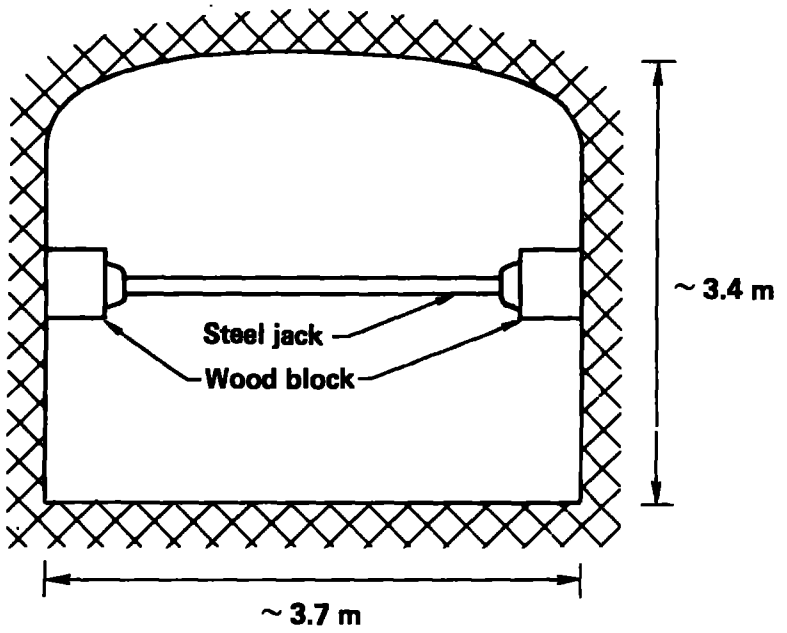

Figure 4. Cross section of drift showing schematically how the wood/jack source was set up. The hammer was swung in and out of the plane of the page and struck the wood block.

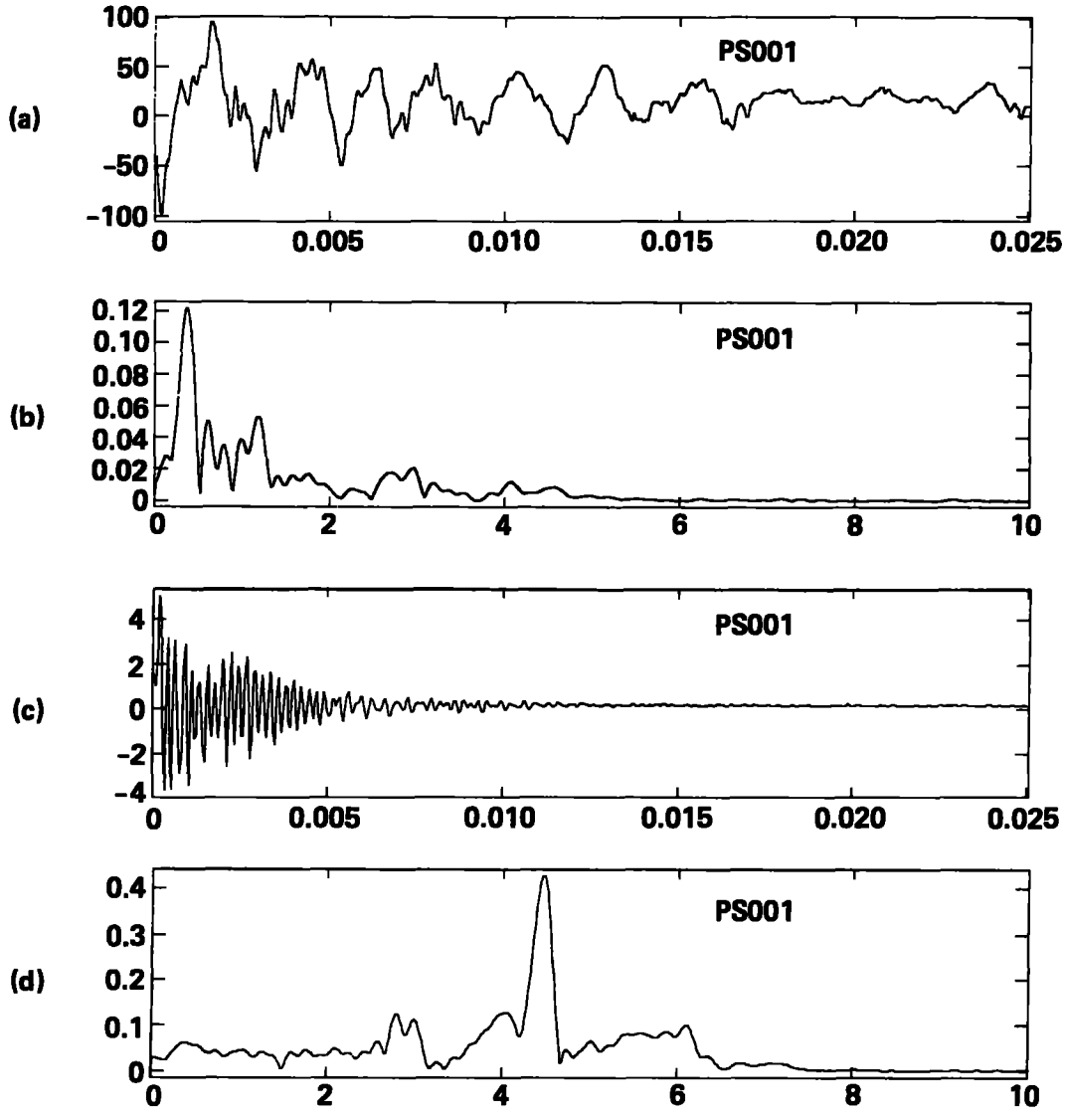

Figure 5. Time and frequency domain plots of signals recorded directly next to the source point located at PS01. (a) Time series recorded from wood/jack source; (b) amplitude spectrum of signal in 5a; (c) time series recorded from al-block source; (d) amplitude spectrum of signal in 5c.

is also valid for the model GH-3-14 geophone used in the Heuze et al. (1981) survey. However, Fig. 6 suggests that a peak frequency measured near 1.6 kHz in the first part of this experiment can probably be disregarded because it could indicate that the geophone was resonating.

Figure 7 shows the frequency response of three different GS-11D geophones with critical damping to a constant velocity input (Lepper, 1981). The natural frequency of the model GS-11D geophone is 14 Hz. Note that the response of the GS-11D is relatively flat out to about 2000 Hz, where the response begins to peak. After the peak, the response falls off rapidly with only a minor peak breaking the trend. By 10,000 Hz, the response of the geophone is down approximately 36 db. These geophones are well suited to the present study because the peak in the response curve is well above the range of interest.

As a check of Lepper's results, shake-table tests were done on the geophones at the LLNL transducer shop. Lepper's results were reproducible up to 3000 Hz, where the response is almost at its maximum (Fig. 8).

The DYMAC model M81 geophone, which is specifically designed for high frequency operation, was also considered. Figure 9 shows the LLNL shake-table results. The response was quite

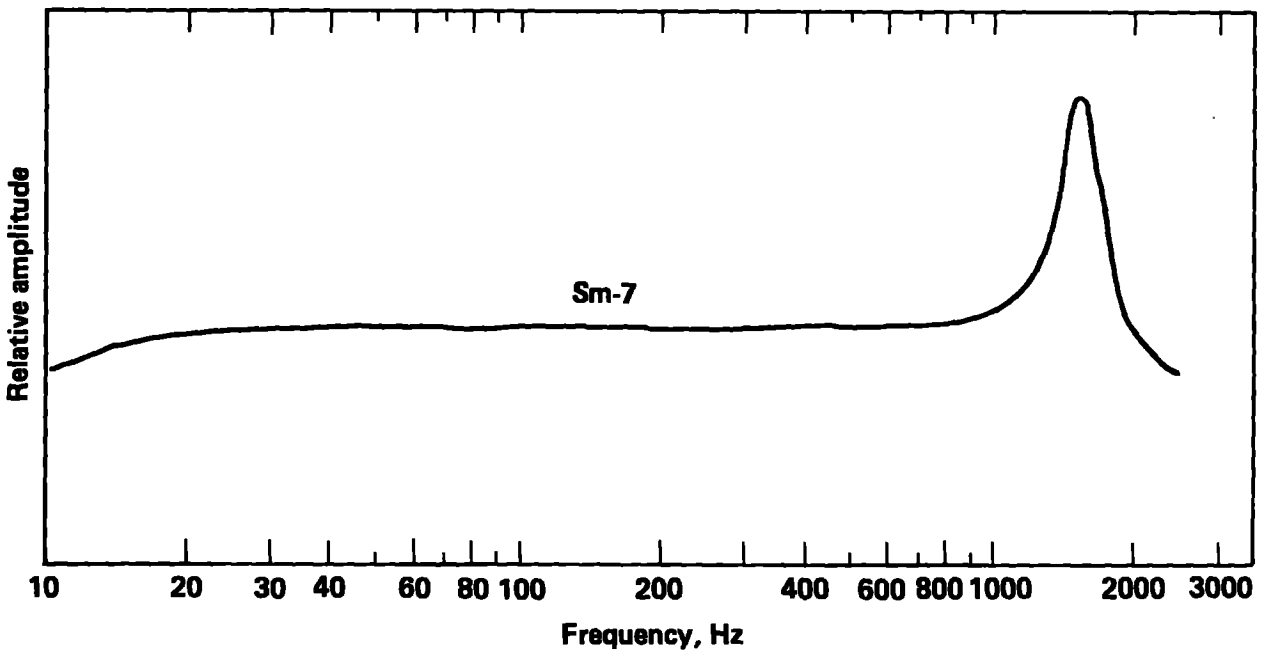

Figure 6. Velocity response of a model SM-7 geophone as measured by LLNL.

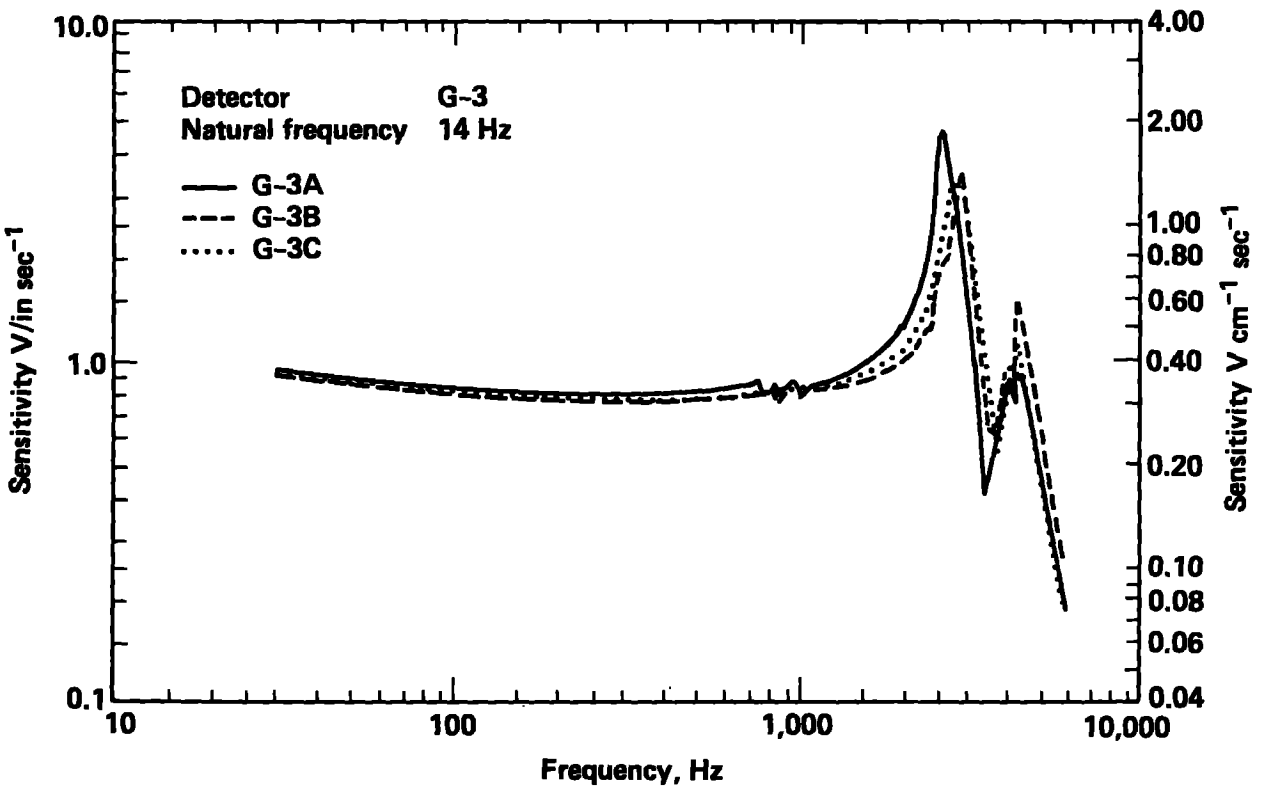

Figure 7. Velocity response of three different model GS-11D geophones (after Lepper, 1981).

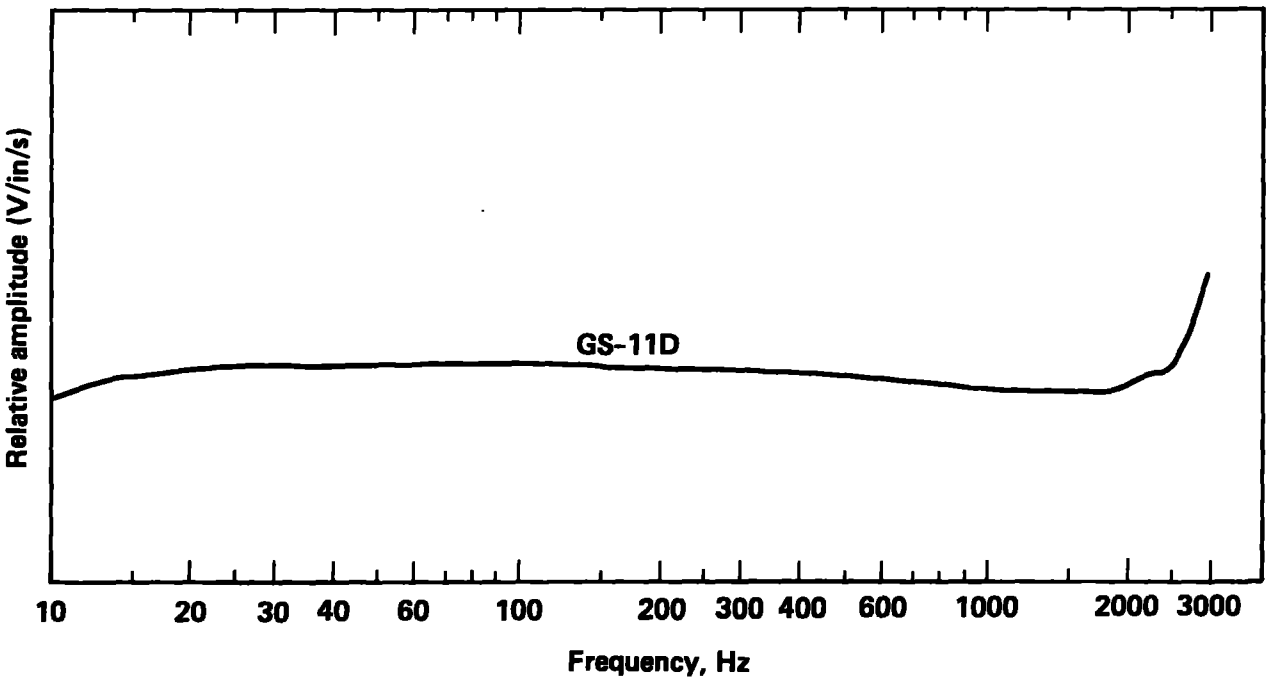

Figure 8. Velocity response of a model GS-11D geophone measured at the LLNL shake table. Our results are consistent with Lepper's (1981) up to 3000 Hz.

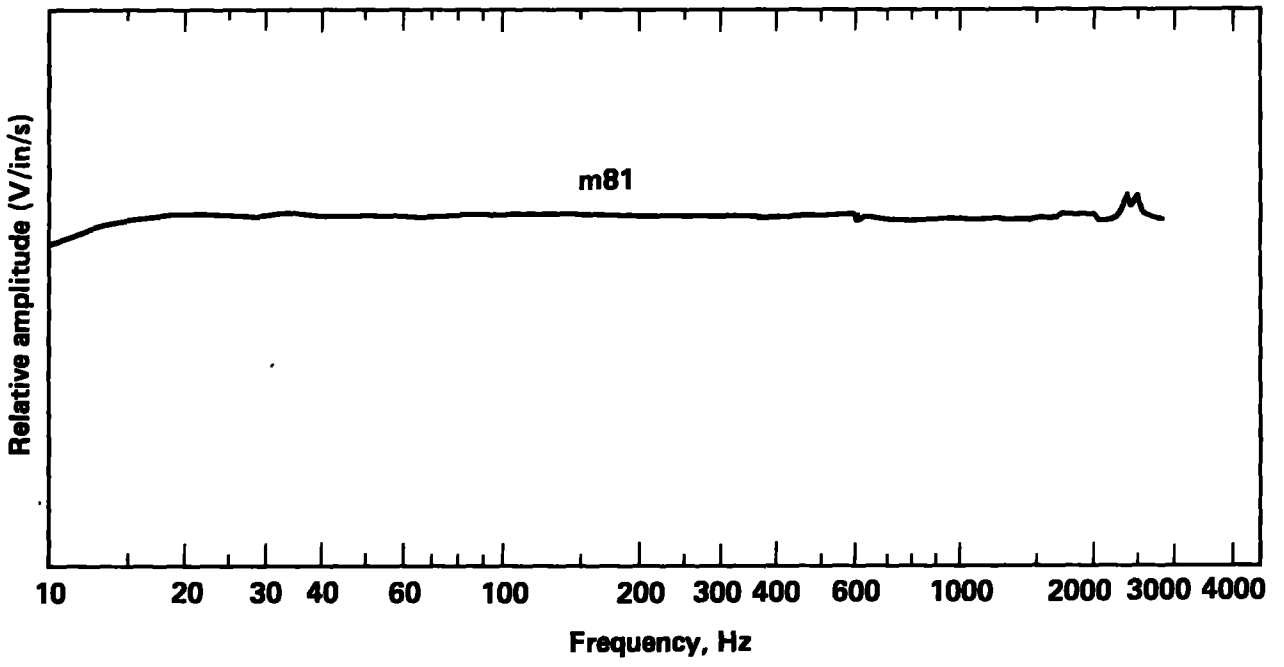

Figure 9. Velocity response of a model M81 geophone as measured at LLNL.

good up to about 3000 Hz. However, the generator constant was much lower than the GS-11D. The M81 was tested in the field but the data were not used because the low generator constant made it difficult to obtain a good signal-to-noise ratio.

Experimental Results

The data coming into the seismograph from the geophone string are first amplified and filtered and then passed to the analog-to-digital converter. The factory amplifier circuits act as a low-pass filter with a corner frequency of 800 Hz. This was too low for the purposes of this experiment so the amplifiers were modified to increase the frequency response. This action produced a flat amplifier response past 10,000 Hz for low amplifications. For higher amplifications, the corner frequency decreased to a limit of approximately 3000 Hz. However, the field calibrations show that the amplifier noise at the high amplifications is enough to degrade the signal to the point that it is unusable. The degradation of the signal was easily identifiable by a visually recognizable reduction in signal quality as a result of saturation of the signal by high-frequency noise.

The seismograph was operated throughout the field operation with a sweep time of 50 ms. The record length of the seismograph was fixed at 1024 samples/channel/sweep, which gives a nyquist frequency of 10,000 Hz. The nyquist frequency is an important parameter of the digital sampling of an analog signal. Frequencies above the nyquist frequency will fold down into the frequencies below the nyquist and "alias" the data, i.e., amplitudes will appear on the amplitude spectra that should not be there. Aliasing is avoided by passing the analog signal through a low-pass filter before the digital sampling. In our case, the modification of the input amplifiers was such that the low-pass filtering effect of the input amplifiers occurred above the nyquist frequency. This implies that there are possible aliasing problems at the low gain settings. However, I believe that aliasing does not produce a problem within data for the following reasons. Figure 10 illustrates the primary reason. The figure shows the plot of the spectra of the whole seismogram that was recorded directly next to source point PS01 with the wood/jack source type and a model GS-11D geophone. The amplitude falls off at high frequencies at a rate of 15 db/octave, with a corner at 400 Hz. The peak in the spectra at 400 Hz is the main spectral peak in the data. The local peak in the spectra at 2500 Hz is due to the peak in the response curve of the geophone. At the nyquist frequency of 10,000 Hz, the signal is down about 65 db, which implies that the signal is band-limited and, therefore, not aliased. Furthermore, the response of the geophone itself rolls off quite sharply at high frequencies (Fig. 7), which also band-limits the signal. I conclude that aliasing is not a problem, even though an anti-aliasing filter was not applied.

The field tapes were played back in the office into a Prime 750 computer. The first step in the processing was to pick the S-arrival time and also the P-arrival times where appropriate. The criteria for identifying an S-arrival is an abrupt change in amplitude that is sometimes accompanied by a change to lower frequencies. The P-arrival is easier to identify because it is the first wave to arrive. It is identified by a sudden increase in the signal above the background noise.

After the P- and S-arrivals had been identified, the P- and S-wave velocities were calculated using the length of the travel path measured by an optical surveying technique.

The spectra for the S-wave was calculated by removing a 6-ms segment of the signal, starting at the S-arrival. The segment or "window" was then multiplied by a cosine taper that brings the ends of the window smoothly to zero. The fast Fourier transform was taken and the results plotted in a linear-linear format. The peak (or dominant) value of the spectra was picked from these results.

Figure 11 shows all the successfully recorded data for the first part of the experiment. The S-wave arrival times are indicated by an arrow, as is the dominant frequency of the S-wavelet in the corresponding plot of the spectra. Refer to Fig. 2a for source and receiver locations. Note that the S-wave can be difficult to identify on some of the records when the source and receiver are close together. The problem is that the P- and S-waves have not traveled a long enough path to allow them to separate in time to become individually identifiable. For example, consider a 500-Hz S-wave traveling at 3.05 km/s and a 500-Hz P-wave traveling at 5.70 km/s. At 10 m from the source the P-wave is 1.52 ms ahead of the S-wave. This means that the S-wave arrives approximately

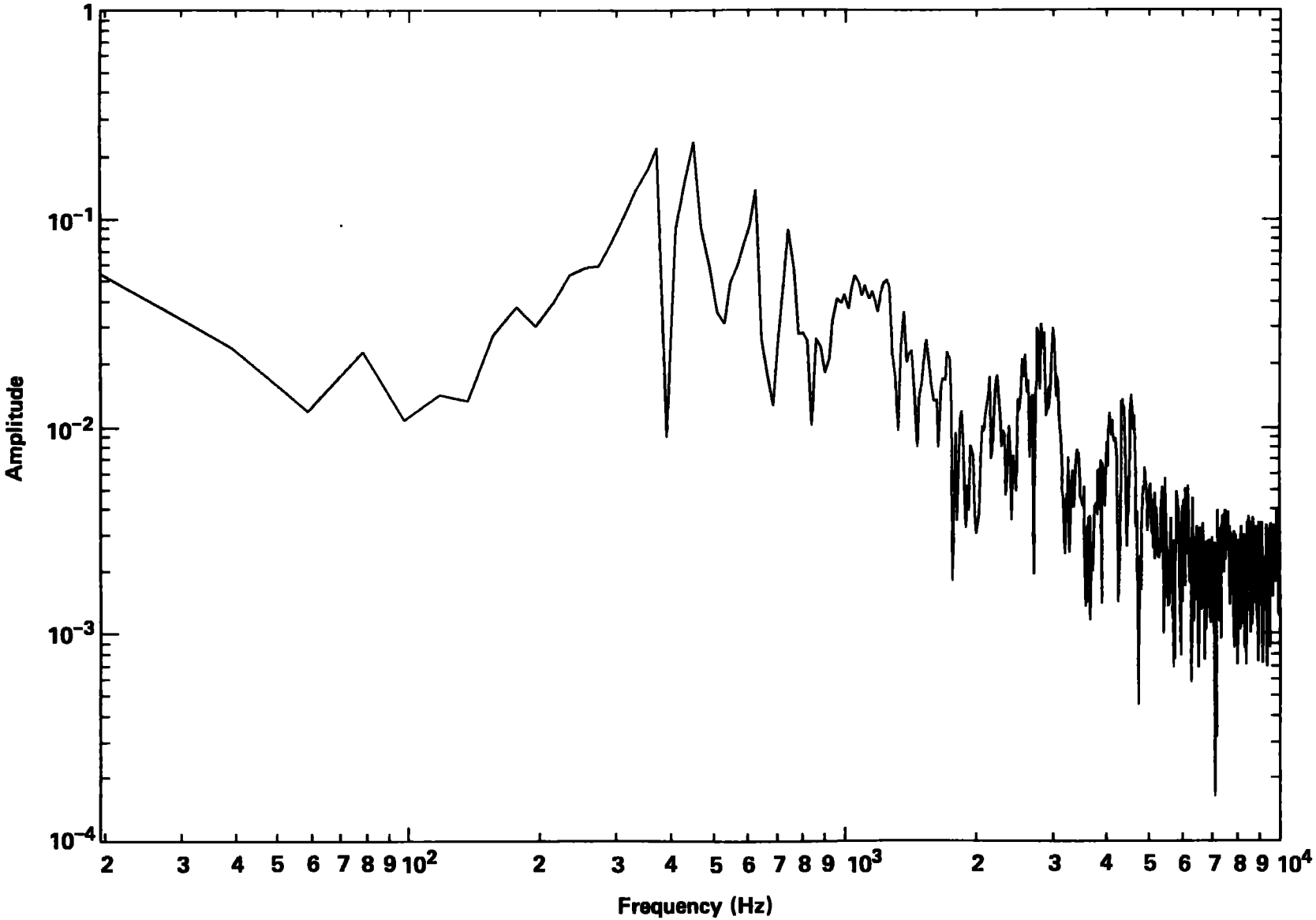

Figure 10. Log-log spectra of the signal recorded at the geophone directly next to source PS13 (wood/jack). Note the roll-off of energy to the higher frequencies and the local peak in the spectra at 2500 Hz.

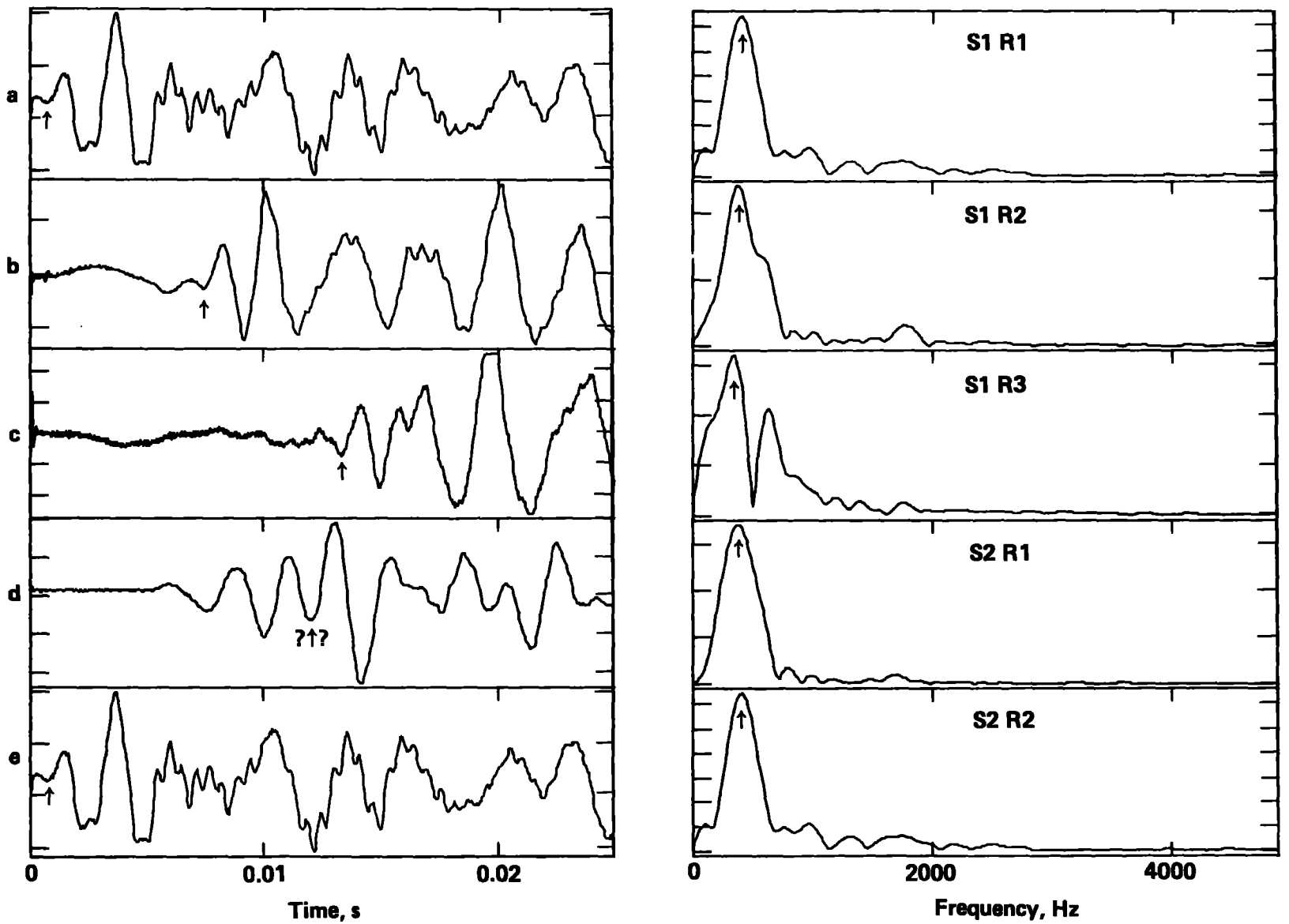

Figure 11a-e. Signal-spectra pairs for the first part of the experiment. The spectra are plotted in a linear-linear format. The S-wave arrival time picks are indicated by arrows, as are the picks of the peak frequency. The window length for the S-wave is 6 ms after the onset.

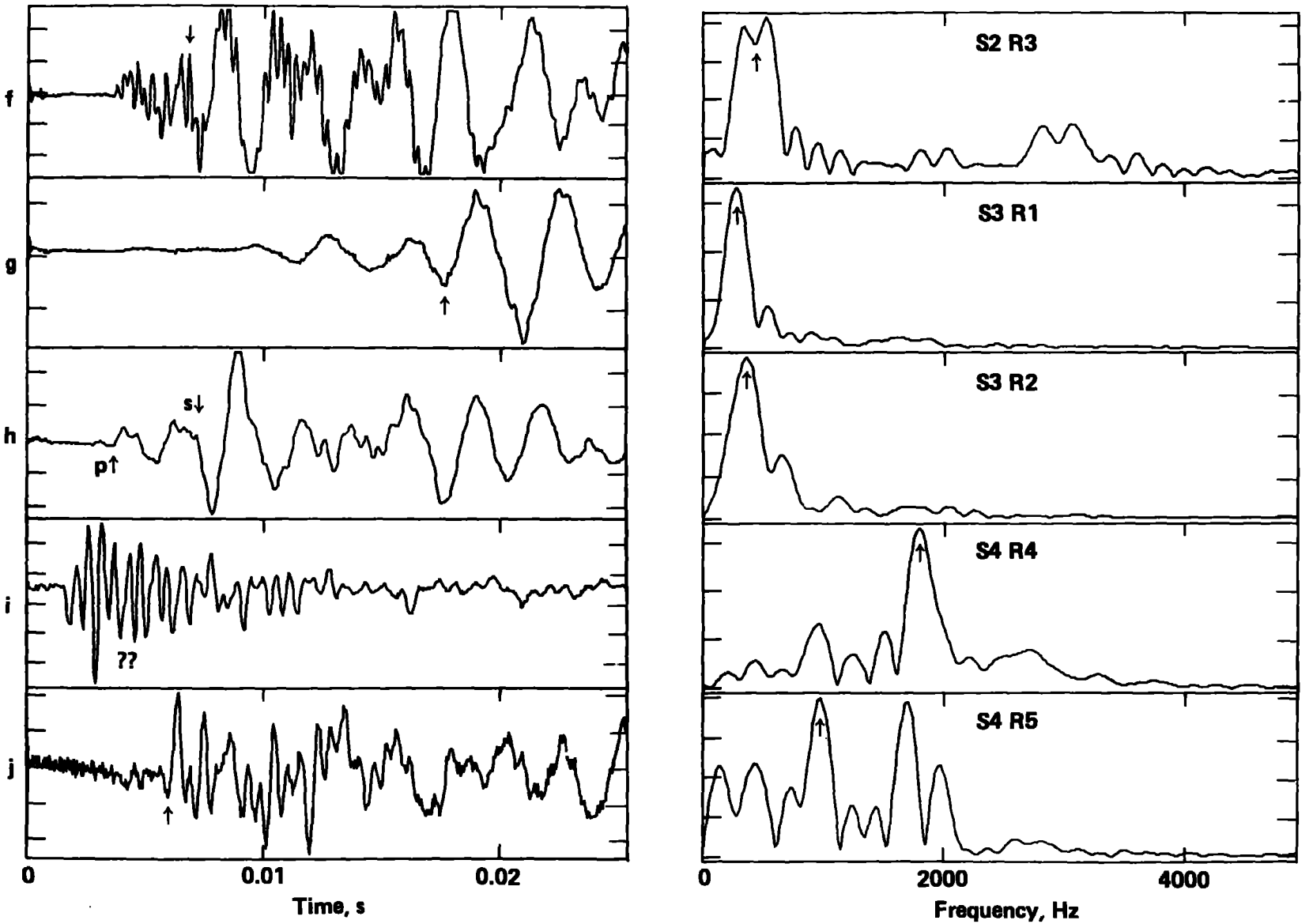

Figure 11a–s. (Continued.)

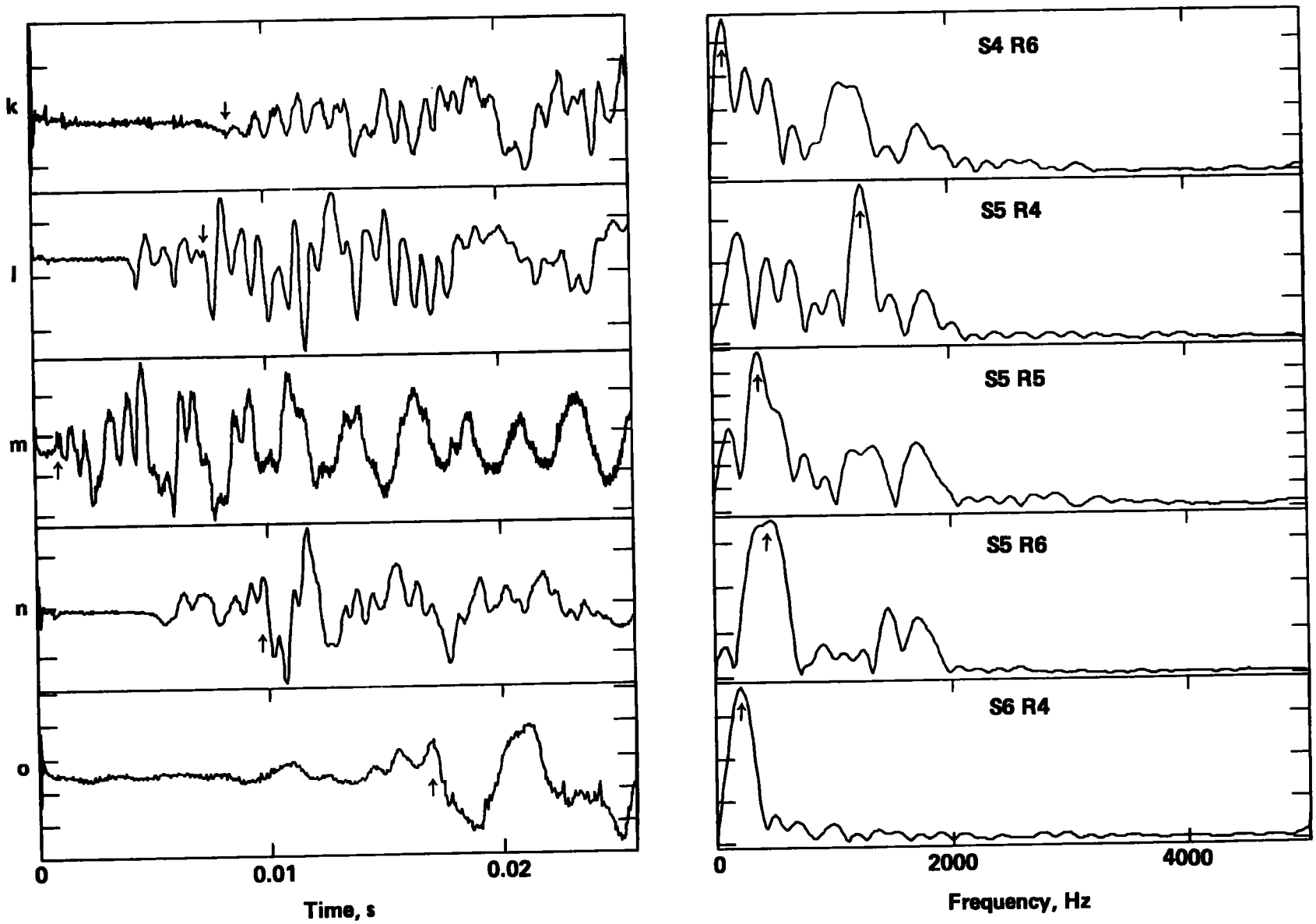

Figure 11a–s. (Continued.)

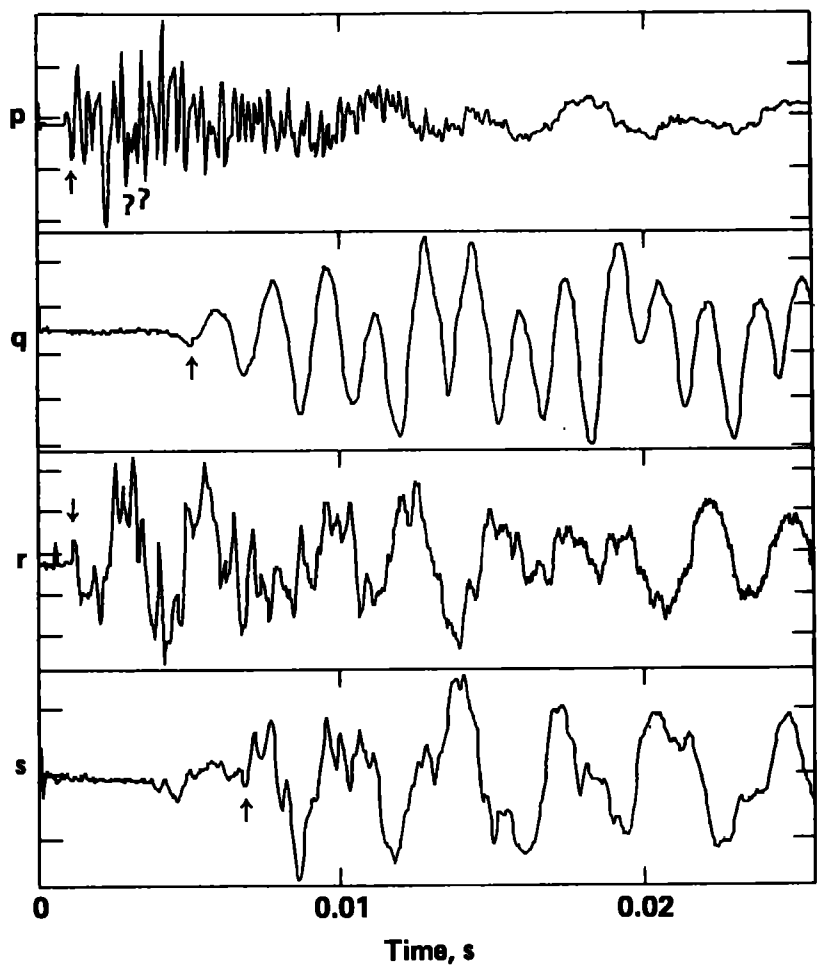

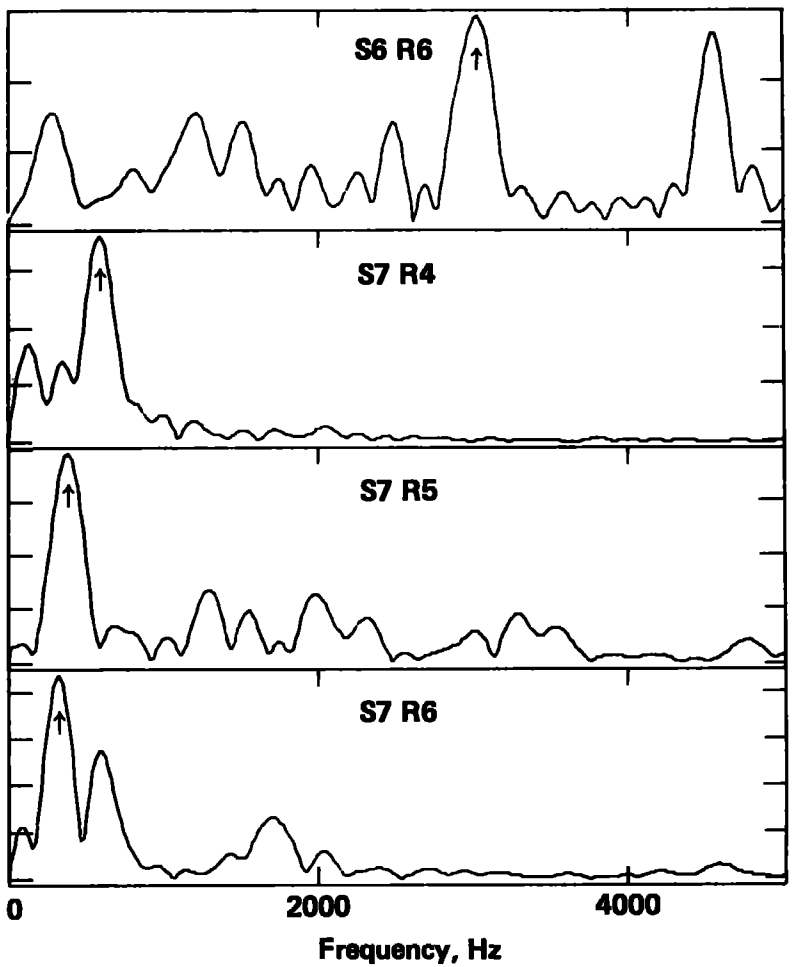

Figure 11a–s. (Continued.)

three-quarters of a period behind the P-wave. Qualitatively, this is roughly the minimum separation in time that will allow the two arrivals to be identified by eye. Another reason why the S-wave can sometimes be difficult to identify is because the geophone polarity switch did not adequately suppress the P-wave. Figure 11a illustrates the above points. The source–receiver separation is less than 10 m and the S-wave arrives on top of the P-wave. Figure 11h shows how a distinct P-wave is developed even though the polarity-reversing switch was used. Figure 12 shows the histogram of the dominant shear-wave frequency for the first part of the experiment. The mean of the distribution is 360 Hz and the standard deviation is 100 Hz.

For the second part of the experiment, the geophones were set out in an 11-station array on both sides of the canister drift. The source points were located in the heater drifts (Fig. 2b). The twelfth channel recorded a geophone that was placed within 1 m of the source, which is within one-half of a wavelength for the peak frequencies recorded, so that an accurate representation of the source signal could be obtained.

The data from the four wood/jack sources are shown in Figs. 13 to 16. The data from source location PS15 for the al-block are shown in Fig. 17. In general, the data from the al-blocks were poor because they were too small to hit sharply enough to impart sufficient energy into the rock. As a result, the gains had to be set very high on the seismograph, and amplifier noise contaminated the signal. Figure 17 is included as an example to show the quality of these data.

The S-wave arrival can be clearly identified on most of the traces in the record sections of Figs. 13 through 16. Besides the above criteria for identifying the S-wave arrival, the S-wave travel-time branch can also be used when the data are

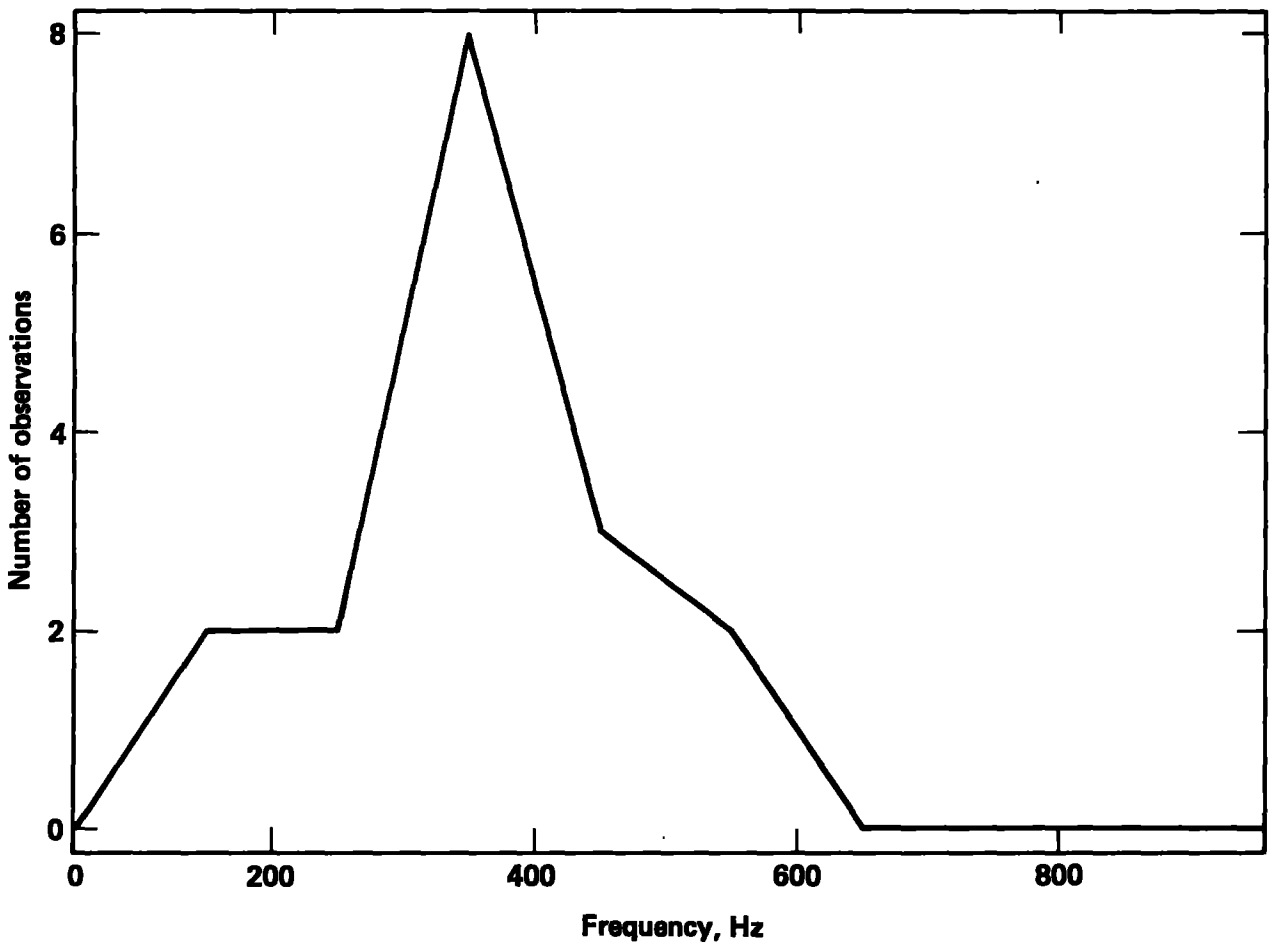

Figure 12. Histogram of peak frequency observations taken from Fig. 9. The total number of observations is 18. The bin size is 100 Hz. The mean of the data is 360 Hz and the standard deviation is 110 Hz.

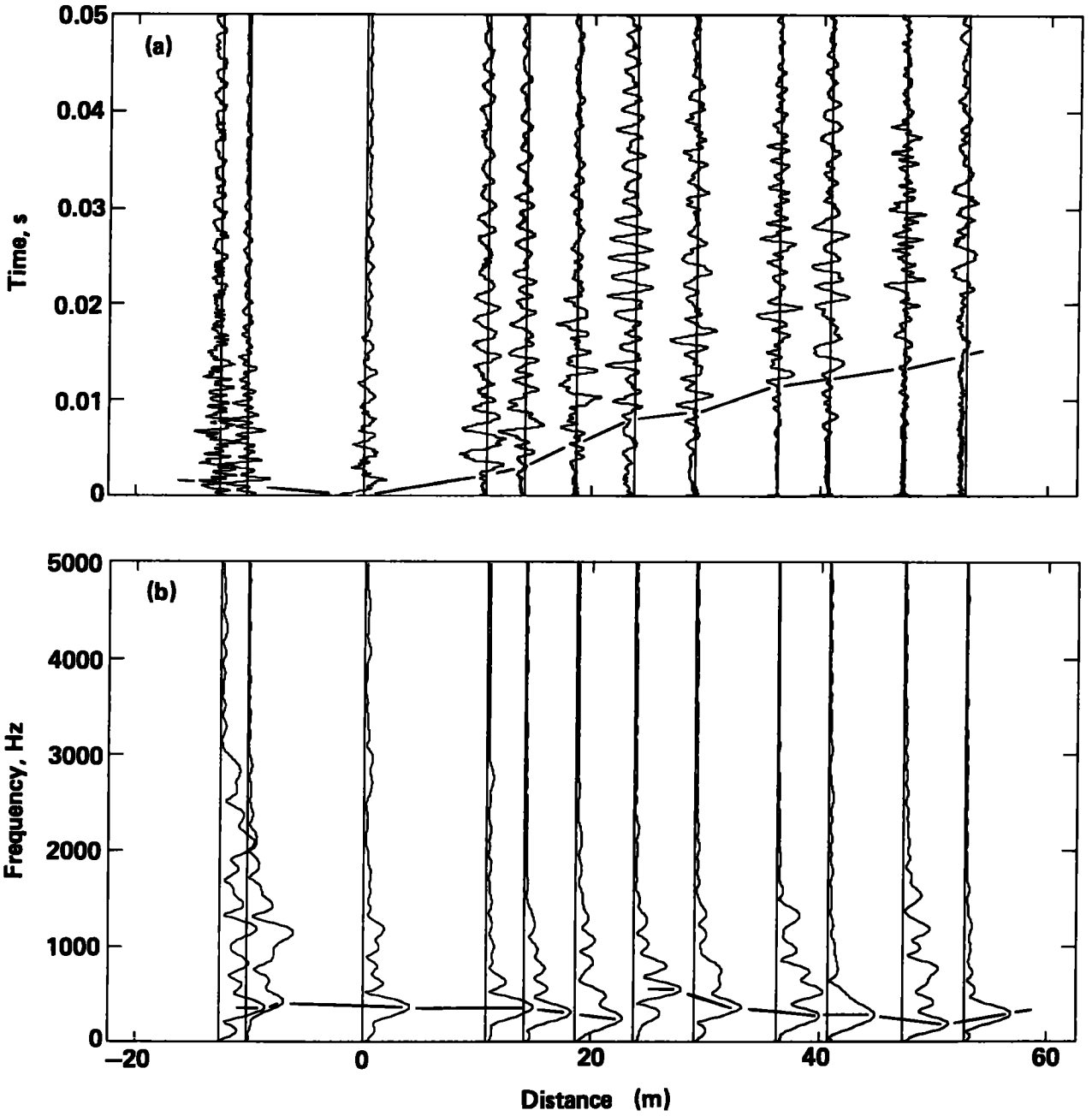

Figure 13. Data for source point PS01 from wood/jack source. (a) Record section of raw seismograms. The solid line indicates the S-wave travel time curve and, hence, the S-wave arrival time pick; (b) spectra for windowed S-wave. The window length is 6 ms. The peak frequency pick is indicated by an arrow and arrow with question marks where uncertain.

viewed in the record section. In this case, the trace is plotted at its actual distance and time from the source. The arrival at a poor quality trace can be estimated if good quality traces surround it. The S-wave arrival time was estimated in this manner for the short travel paths where the P- and S-wave arrivals were not clearly separated in time.

As was discovered in the first part of the experiment, the geophone polarity reversing switch was not very effective in cancelling the P-wave. The P-wave can be clearly identified on most of the traces shown in Figs. 13 through 16.

Plotted with each record section is another record section of the spectra. In general, most of the energy excited by the wood/jack source is less

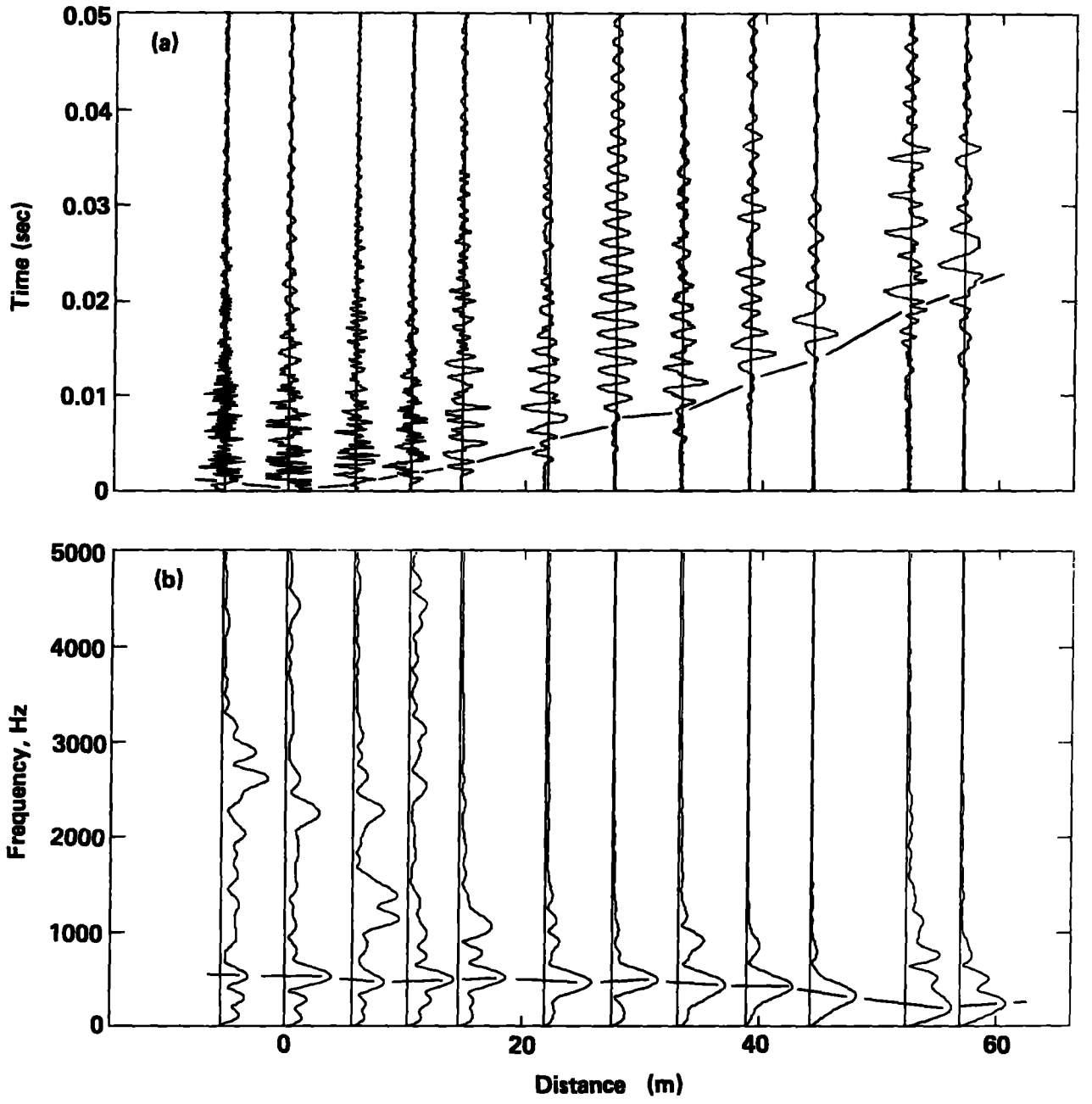

Figure 14. Same as Fig. 11, except for source point PS13.

than 1000 Hz in frequency. However, for some recordings, especially those near the source, the spectra show peaks around 2100–2200 Hz. These result from the resonance of the geophone and are not being excited in the rock to the degree shown in the spectra. The al-block clearly excited higher frequencies than the wood/jack, but the frequencies were near the peak in the response spectra of the geophone, making the data unreliable (Fig. 17b vs Fig. 13b). However, it is clear from these data that the lower frequencies were not being excited to the same extent as with the wood/jack.

The P- and S-wave arrival times were all picked and the P- and S-wave velocities were

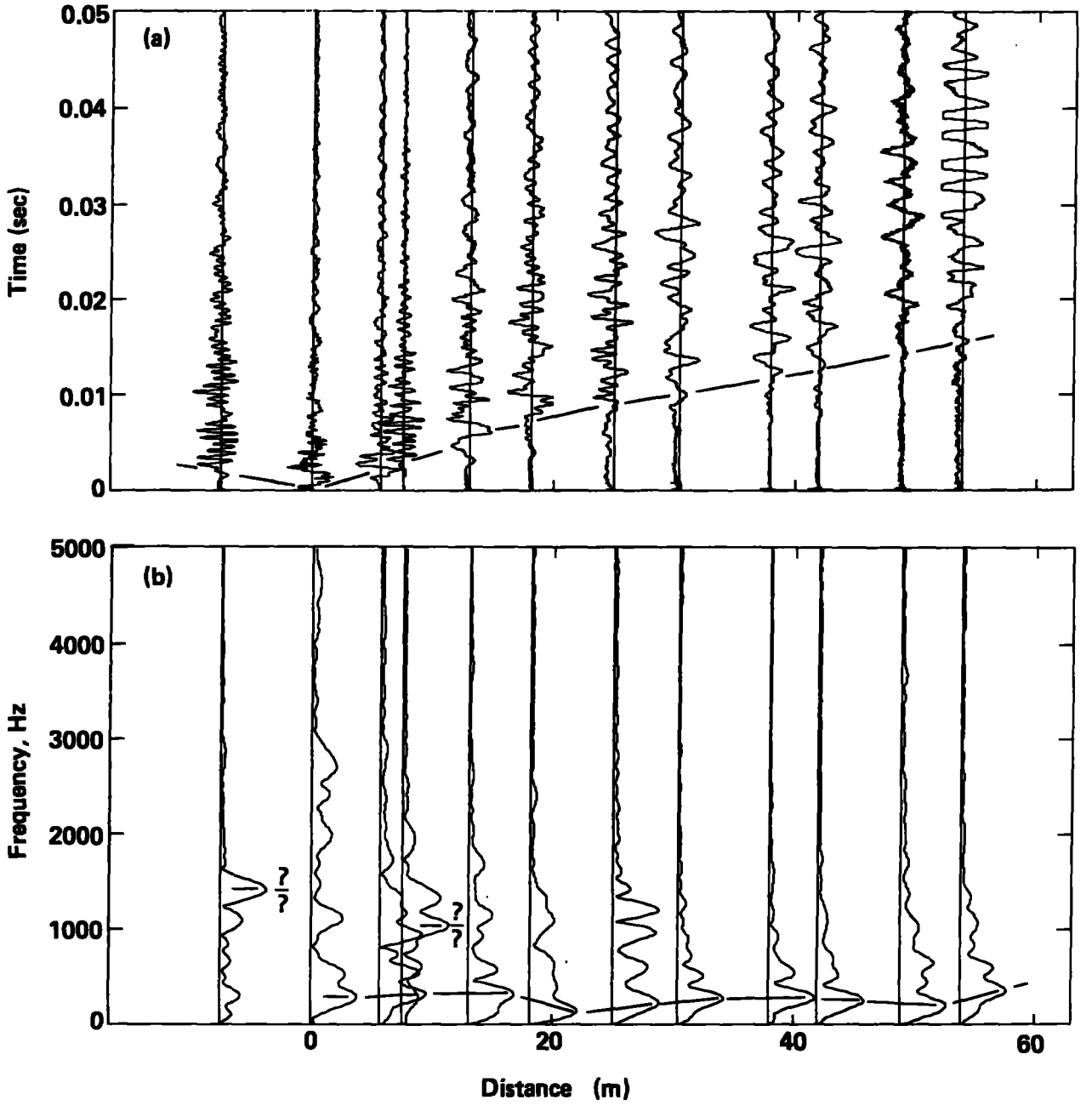

Figure 15. Same as Fig. 11, except for source point PS14.

computed. Figure 18a shows the distribution of Vp (P-wave velocity) from a total of 99 observations. The mean Vp is 5.9 km/s, but the mode is 5.6 km/s, which indicates that the distribution is mildly skewed to the higher velocities. Figure 18b shows a similar plot for Vs (S-wave velocities) from a total of 83 observations. The mean of the Vs distribution is 3.1 km/s and the mode is 3.05 km/s, which indicates a mild bias toward higher velocities, but is probably not significant given the variability of the data.

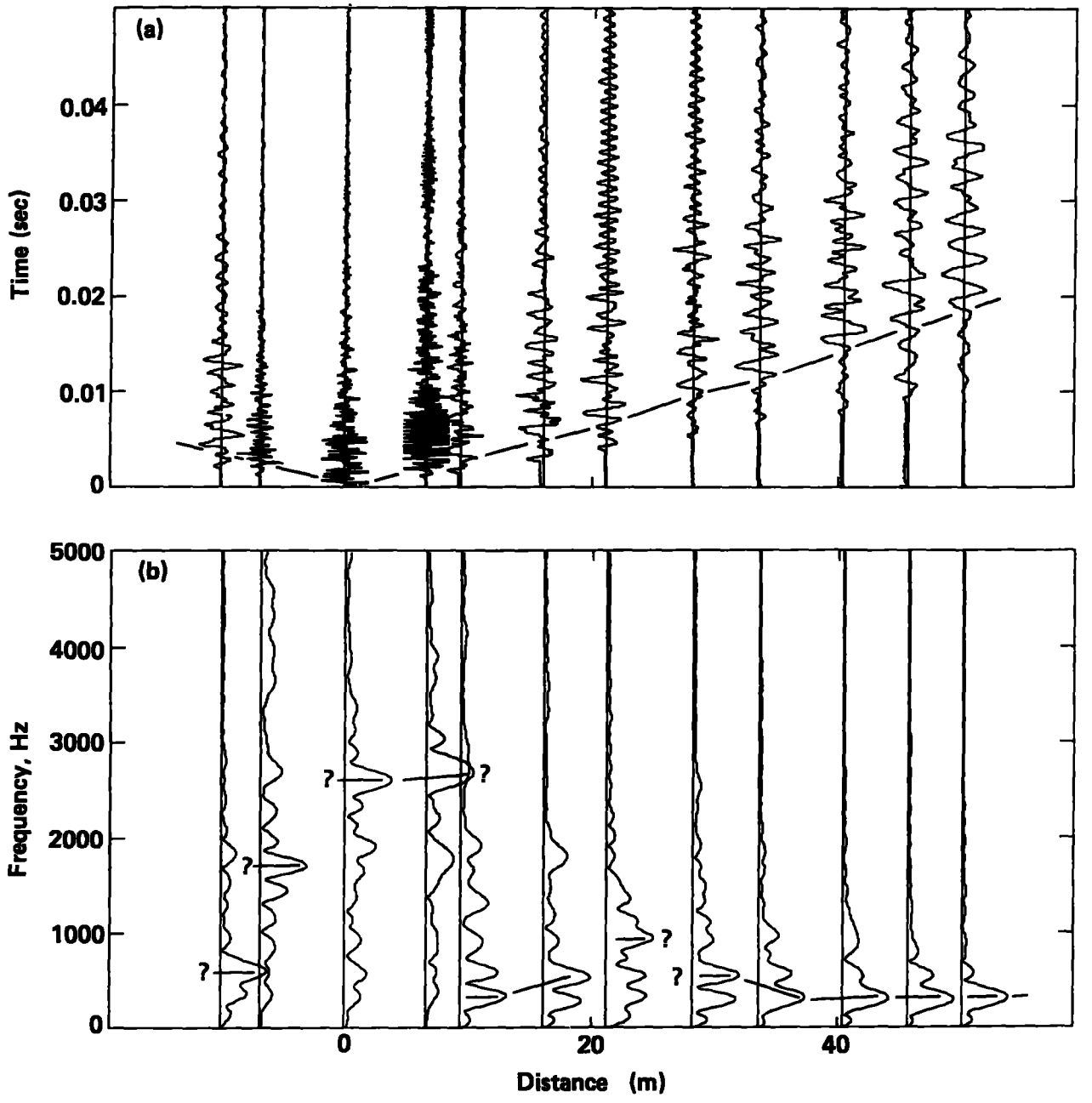

Figure 16. Same as Fig. 11, except for source point PS15.

Discussion

The Vp and Vs data can be used to calculate the dynamic modulus of the rock (Jaeger and Cook, 1969, p. 172), such that

$$E_d = V_s^2 \rho \frac{3V_p^2/V_s^2 - 4}{V_p^2/V_s^2 - 1}$$

where ρ = density [a value of 2.63 g/cc was used (Patrick and Mayr, 1981)].

The dynamic Poisson's ratio may also be calculated (ibid):

$$\nu_d = \frac{1}{2}\left[\frac{V_p^2/V_s^2 - 2}{V_p^2/V_s^2 - 1}\right]$$

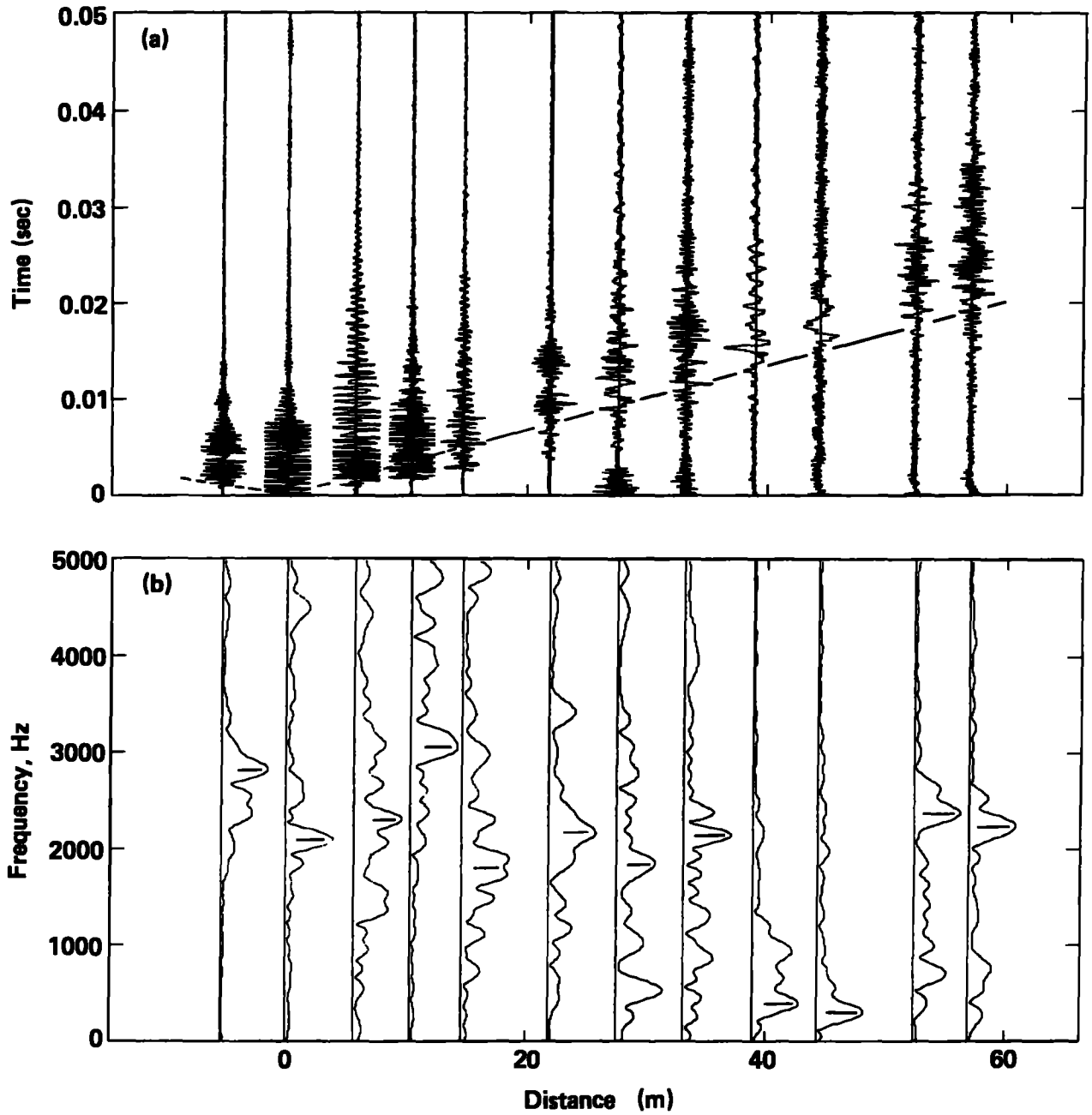

Figure 17. Same as Fig. 11, except for source point PS13 with the al-block source rather than the wood/jack.

This method of determining the deformability constant has been known for some time, and has received some renewed attention recently (Aikas et al., 1983). The main problem with the method is that it measures E for transient, small-amplitude deformations. When calculating rock mass response to excavation or heating, the *in-situ*, static modulus is the more appropriate value to use. The dynamic modulus is normally higher than the static modulus (Jaeger and Cook, 1969). It is a point of research to find the reduction factor that tranforms the dynamic modulus into the static modulus for any specific rock mass (c.f., Heuze et al., 1981).

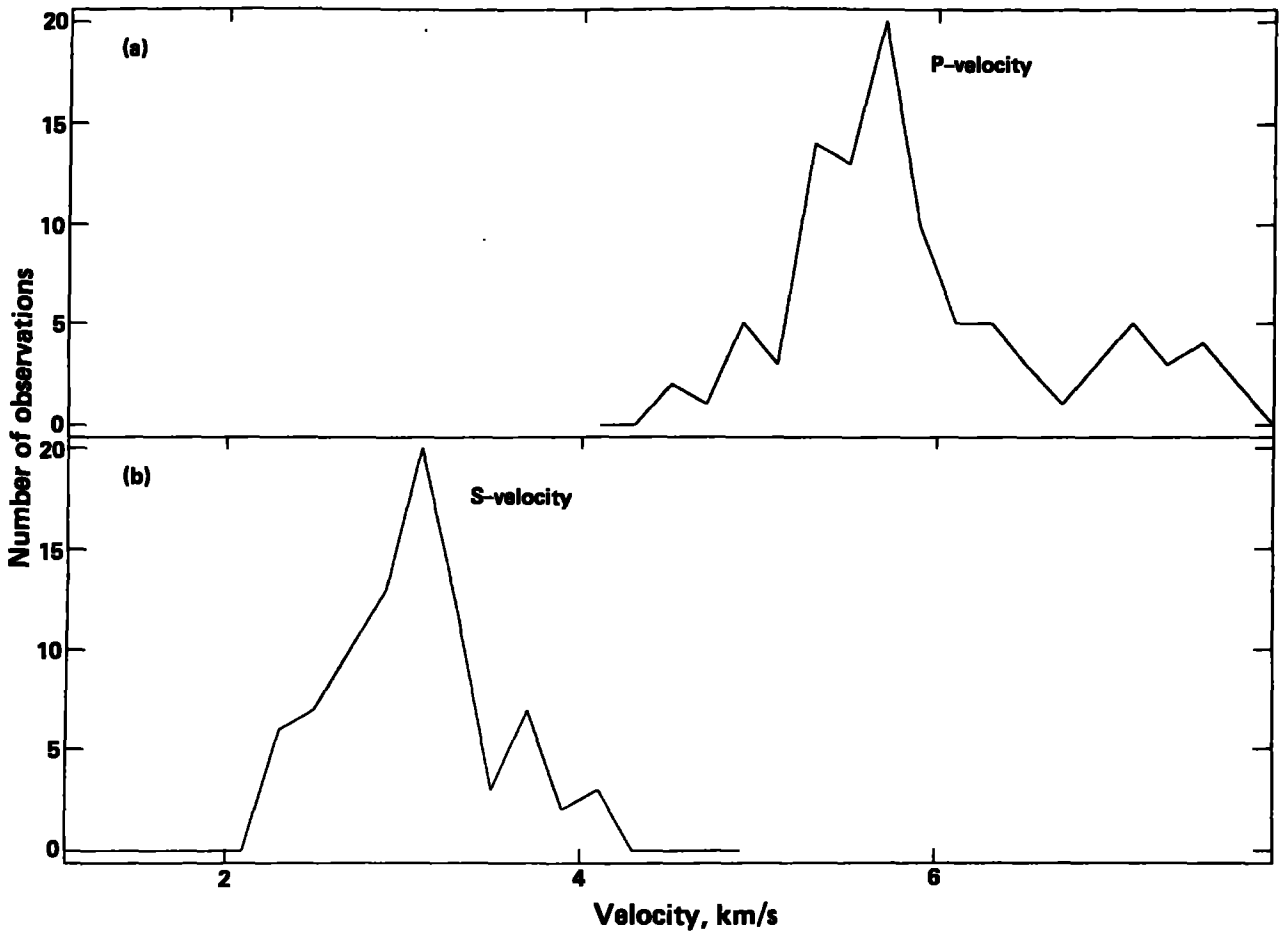

Figure 18. (a) Histogram of P-wave velocity (Vp) measurement, calculated from the data recorded in the second part of the experiment. Not all the data used in this plot could be shown in Figs. 13 through 16. The total number of observations is 82. The bin size is 0.25 km/s. The mean of the ungrouped data is 5.9 km/s and the standard deviation is 0.74 km/s. (b) Histogram of S-wave velocity (Vs) measurements calculated from the data recorded in the second part of the experiment. Not all the data used in this plot could be shown in Figs. 13 through 16. The total number of observations is 84. The bin size is 0.25 km/s. The mean of the ungrouped data is 3.07 km/s and the standard deviation is 0.44 km/s.

From the Vp and Vs data shown in Fig. 18, I calculate a mean E_d* of 61 GPa with a standard deviation of 16 GPa and a mean ν_d of 0.28 with a standard deviation of 0.08. The value of E_d is very close to the average of laboratory measurements of E_s of 70 GPa reported by Heuze et al. (1981). Pratt et al. (1979) has made laboratory measurements of E_d, E_s, ν_d for core samples from SFT—C. My E_d results are somewhat lower than the average E_d of 74 GPa reported by Pratt et al. (ibid). However, the E_d and E_s values compare favorably. It is interesting to note that E_d from the larger cores (143 mm in diameter) have similar E_s and E_d values as reported by Pratt et al. (ibid), whereas the E_s values of the smaller cores (76 mm) are markedly smaller than the E_d values. My measured value of ν_d is somewhat higher than the average ν_d reported by Patrick et al. (ibid) of 0.25.

* E_d and ν_d were calculated by pairing the V_p and V_s values by path. For example the V_p measured for the path PS01 to PS08 was paired with the V_s for the same path. A total number of 57 and 58 pairs were used to calculate ν_d and E_d, respectively.

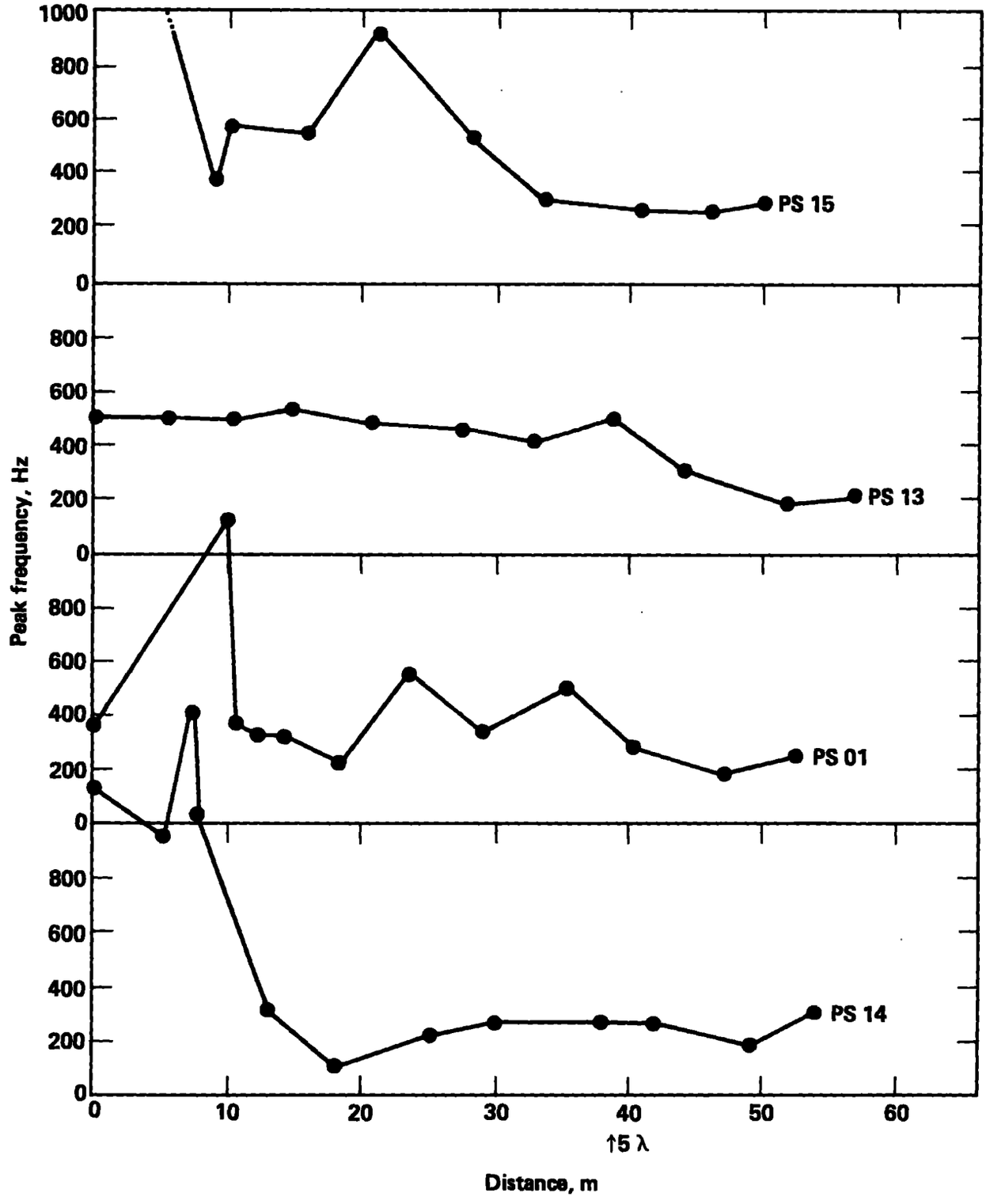

Figure 19. Peak-frequency vs distance from the source for the data in Figs. 11b through 14b. The five-wavelength (5λ) point for a 500 Hz wave is shown at 38 m.

From the first part of the experiment, I measured a peak frequency of 360 Hz, which corresponds to modulus of 8 GPa when using the empirical relationship shown in Fig. 1. Heuze et al. (1981) measure a peak frequency of 1100 Hz, which corresponds to a modulus of 50 GPa. This indicates a reduction of the modulus, over the duration of the spent fuel test, from 50 to 8 GPa, or 87%. For reasons discussed below, this is probably not a real change; there is good reason to suspect that the petite sismique method produces severely biased results.

Figure 19 summarizes the data from the wood/jack source. In the figure, the spectral peaks are plotted against distance from the source. A general feature of these curves is that the peak frequency starts out high and begins to fall off after some distance. By 40 m from the source, all four curves have dropped at least below 500 Hz. Thus, the rock appears to be behaving as a low-pass filter.

Figure 20 shows the same type of plot for the al-block source. These data are erratic and difficult to interpret. There seems to be an actual increase

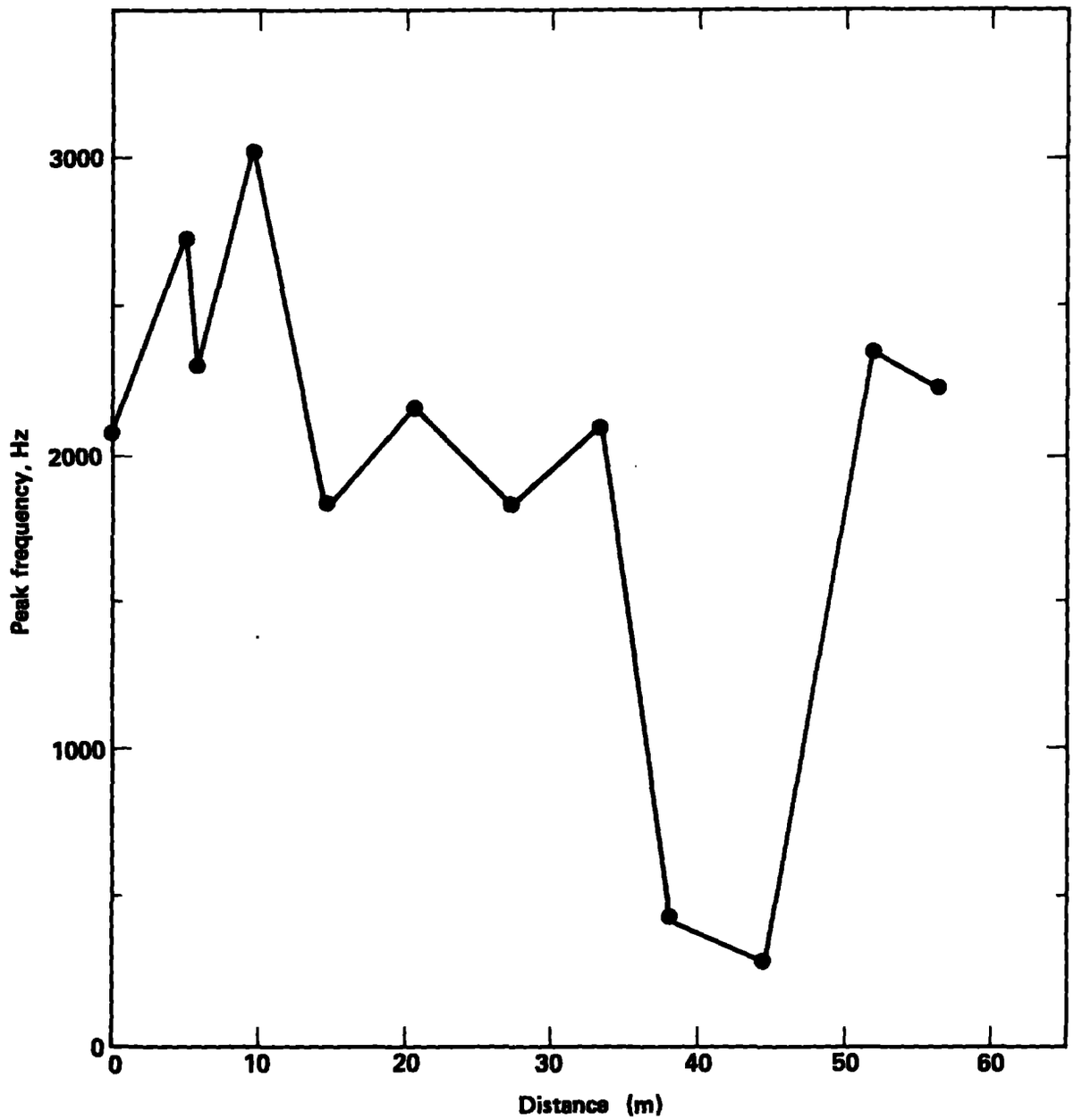

Figure 20. Peak-frequency vs distance from the source for the data in Fig. 15.

in peak frequency away from the source for the first 10 m. Then the peak frequency levels off at approximately 2000 Hz for the remainder of the stations, except for two stations at distances of 38 and 45 km. The al-block source was not as energetic as the wood/jack source and because of this, the gain settings had to be set quite high, which probably introduced amplifier noise into the signal. Therefore, the results at distances greater than 40 km, where the higher gain settings were used, are probably unreliable.

Comparisons of Figs. 19 and 20, and 5b and 5d show that the different sources excite different frequencies in the rock. The al-block source clearly imparts higher frequency energy into the rock. This means that the hammer blow is not impulsive, i.e., a flat spectrum of frequencies is not being produced at the source, or more precisely, the transfer function of the source varies with the type of source. The wood transfers the frequencies generated by the hammer blow differently than aluminum. Wood is a more attenuative material than aluminum, so it would tend to transfer lower frequencies than the aluminum. The results of this study show that the peak frequency measured at a given distance from the source will depend on the source and the distance. The original papers on the petite sismique technique (Schneider, 1967; Bieniawski, 1978) did not discuss either the spectral qualities of the source or the dependence of peak frequency on path length. Until these effects can be incorporated into the empirical relationship in Fig. 1, I feel that the petite sismique technique does not produce reliable results.

In recent experiments that are similar to petite sismique measurements, Young et al. (1979) have noted the low-pass filtering effect of rock on seismic waves. They have measured the attenuation spectra, which is similar to the petite sismique peak frequently, for a rock mass before and after an explosion has been detonated. The work is being carried out in coal mines and the explosions are designed to facilitate the mining of the coal. Young et al. find that the efficiency of the explosion, i.e., the amount of fracturing introduced into the rock, is directly correlated with a decrease in the corner frequency of the low-pass filtering effect of the rock. The technique has not been calibrated, that is, there is no relationship that expresses the degree of fracturing with the value of the corner frequency.

Recommendation

For future work, an experiment could be designed to measure the frequency response of a rock mass very precisely. For example, a piezoelectric source could be used to produce a monochromatic signal that could then be recorded at various distances. The source would then be swept through a frequency range of, say, 100–2000 Hz. This procedure would accurately characterize the frequency response of the rock and the change of this response with distance. The technique could be calibrated by statistically analyzing the rock mass and performing the experiment in many different areas. Then the results would need to be modeled. The final peak frequency would depend in some way on E_s, Q (quality factor, i.e., the intrinsic attenuation of the rock mass), and fracture density. E_s could eventually be determined if Q could be measured independently and if fracture density could be determined and modeled with scattering theory (c.f., Aki and Richards, 1980).

Conclusions

The petite sismique measurements by Heuze et al. (1981) were repeated in two parts, the first of which was a repetition of the earlier experiment. The same source and geophone points were occupied; however, it is not certain if the geophone used in this experiment had the identical response to the geophone used in the previous experiment. The second part of the experiment consisted of deploying a 12-channel array of geophones and two types of sources, with the emphasis on understanding the evolution of the wavefield from the sources and minimizing the effect of resonances inherent in the sources and geophones.

In the first part of the experiment, a dominant shear-wave frequency of 480 Hz was found that is significantly less than the 1100-Hz dominant frequency measured by Heuze et al. (1981). However, this result could be biased by the geophone

response since it is not certain if the frequency response of the GH-3-14 geophone, used in the old study, is equivalent to the response of the SM-7 geophone, used in the first part of this study.

In the second part of the experiment, the rock was found to act like a low-pass filter to the wave train. The low-pass filtering effect becomes evident in the wave field after propagation of approximately 40 m. The blow from the hammer is not a pure impulse, which means that the frequencies excited in the rocks at the source location depend on the type of source used. These two results taken together mean that the peak frequency observed will depend on the distance from the source and the type of source. This result implies that the petite sismique technique could give spurious results depending on the above factors. Research should be done to factor the source and path length effects into the empirical modulus/peak-frequency relationship before the results from a petite sismique measurement can be used with confidence.

Acknowledgments

I would like to thank the many people who contributed to this work. John Scarafiotti provided instrument and technical support in the office and in the field. Basil Baily, EG&G-Las Vegas, also helped in the field. REECO miners George Medina and Glen Chambers provided valuable logistical help in the field. R. Taylor of the LLNL plastics shop was very helpful in formulating and providing on short notice the epoxy used in the field. L. Meisner, W. Shay, and C. Knabe of the LLNL transducer shop were very helpful in doing the shake-table tests of the geophones.

W. Patrick and S. Taylor provided technical in-house reviews of this manuscript. J. Scheimer provided helpful technical assistance.

This work was completed as part of the Spent Fuel Test—Climax. The SFT—C is conducted under the technical direction of the Lawrence Livermore National Laboratory as part of the Department of Energy's Nevada Nuclear Waste Storage Investigations.

References

Aikas, K., P. Loven, and P. Sarkka (1983), "Determination of Rock Modulus of Deformation by Hammer Seismograph," *Bull. Intl. Assn. Eng. Geol.* **26–27.**

Aki, K., and P. G. Richards (1980), *Quantitative Seismology Volume 2,* Theory and Methods (W. H. Freeman and Company), 932 pp.

Bieniawski, Z. T. (1978), "Determining Rock Mass Deformability: Experience from Case Histories," *Int. J. Rock Mech. and Min. Sci.* **15(5), 237–247.**

Heuze, F. E., W. C. Patrick, R. V. De la Cruz, and C. F. Voss (1981), *In-situ geomechanics Climax granite, Nevada Test Site,* Lawrence Livermore National Laboratory, Livermore, CA, UCRL-53076.

Jaeger, J. C. and N. G. W. Cook (1969), *Fundamentals of Rock Mechanics* (Chapman and Hall Ltd.), 515 pp.

Lepper, C. M. (1981), *Guidelines for Selecting Seismic Detectors for High-Resolution Applications,* U.S. Bureau of Mines Reports of Investigations 8599.

Patrick, W. C., and M. C. Mayr (1981), *Excavation and Drilling at a Spent-Fuel Test Facility in Granitic Rock,* Lawrence Livermore National Laboratory, Livermore, CA, UCRL-53227.

Patrick, W. P., L. Ballou, T. Butkovich, R. Carlson, W. Durham, G. Hage, E. Majer, D. Montan, R. Nyholm, N. Rector, D. Wilder, and J. Yow, Jr. (1982), *Spent Fuel Test-Climax Technical Measurements Interim Report FY 81,* Lawrence Livermore National Laboratory, Livermore, CA, UCRL-53294.

Pratt, H., R. Lingle, and T. Schrauf (1979), *Laboratory-Measured Material Properties of Quartz Monzonite, Climax Stock, Nevada Test Site,* Terra Tek, Inc. Contractor Report, Lawrence Livermore National Laboratory, Livermore, CA, UCRL-15073.

Schneider (1967), "Moyens Nouveaux de Reconnaissance des Massifs Rocheux" (New Tools for Exploration of Rock Masses), *Ann. Inst. Tech. Batim. Trav. Publics* **62,** 1055–1094.

Young, R. P., J. R. Coffey, and J. J. Hill (1979), "The Application of Spectral Analysis to Rock Quality Evaluation for Mapping Purposes," *Bull. Intl. Assn. Eng. Geol.* **19,** 268–274.